Molecular Docking and Dynamics Simulation study for Anticancer Phytoconstituents inhibiting breast cancer

Singh Nootan[1], Yadav Piyush Kumar[2], Singh Ajay Kumar[2], Gupta Divya[1,3*] and Gupta Garima[1*]
1. Faculty of Biosciences, Institute of Biosciences and Technology, Shri Ramswaroop Memorial University, Lucknow-Deva Road, Barabanki 225003, Uttar Pradesh, INDIA
2. Department of Bioinformatics, Central University of South Bihar, Gaya 823001, Bihar, INDIA
3. Division of Endocrinology and Metabolism, Department of Medicine, University of Pittsburgh, Pittsburgh, Pennsylvania, UNITED STATES
*guptadivya06@gmail.com; garimasumi@gmail.com

Abstract

The main challenge in the fight against breast cancer (BC) is to create new medications that are more selective for cancer cells and have fewer adverse effects. SPDEF (Sam pointed domain containing ETS transcription factor) is a prostate-derived ETS factor that maintains homeostasis, differentiation of epithelial tissues and heritable alterations in cancer. Previously, SPDEF has been shown to be associated with BC subtypes and is found to be down-regulated in invasive breast cancer cell lines which is supportive of its role in tumor suppression. In the current study, SPDEF protein was used as a potential breast cancer therapeutic target. A total of fifteen phytoconstituents were evaluated as potential drug ligands against SPDEF using various in silico approaches. Genistein, allicin, 2-hydroxychalcone and ajoene were free from any of the predicted toxicological endpoints.

As per toxicological endpoints prediction study, the median lethal dosage (LD50) values for these phytoconstituents varied from 159 to 3919 mg/Kg. Our results indicate that out of fifteen, three phytoconstituents silibinin (-7.7 kcal/mol), codonolactone (-6.1 kcal/mol) and genistein (-6.1 kcal/mol), showing the lowest binding energies, had more significant inhibitory effects against SPDEF protein. We selected these three phytoconstituents on the basis of binding scores for molecular dynamic simulations at 200 ns to study their protein-ligand complex stability. Out of the three, silibinin-receptor complex had more stability. The present analysis shows that silibinin could be a potential therapeutic compound against breast cancer as assessed by its binding interaction and stability analyses against SPDEF.

Keywords: Breast cancer, SPDEF, Phytoconstituents, ADMET, Molecular docking and simulation studies.

Introduction

Breast cancer (BC) is one of the most common malignancies diagnosed and the fifth leading cause of cancer-related fatalities. The expanding population and fast ageing process are expected to increase the number of new breast cancer cases to over 3 million and 1 million deaths per year by 2040[10]. Globally, women are more prone to breast cancer than any other type of cancer and it is a disease with various molecular components[46].

BC is clinically divided into four categories based on immunohistochemical traits: triple-negative breast cancer (TNBC), human epidermal growth factor receptor 2 (HER2) overexpression type, luminal A type and luminal B type. Some of the breast cancers are inherited. Specific genetic abnormalities or mutations connected to breast cancer can be found by genetic testing. Several gene mutations have been reported in increased risk of BC progression. BRCA1 and BRCA2 are the two most significant BC susceptible genes located on chromosome 17 and 13 respectively[41]. Both BRCA1 and BRCA2 are involved in DNA repair process. The lifetime chances of developing breast cancer are 72% and 69% for BRCA1 mutant carriers and BRCA2 mutation carriers respectively[4].

Additional genes like TP53, PTEN, CDH1, STK11 and PALB2 may also be involved in BC induction upon interaction with BRCA genes. It is possible to test people who have a family history of breast cancer or who exhibit certain clinical traits that could point to a genetic risk. BC development is also influenced by a number of environmental and lifestyle factors[23]. There are several other genes known to be involved in breast cancer progression like TRIM3, ABCB9, SPDEF, HSPB1, RHBG, SPINT1, EPN3, LRFN2, PRPH etc.[53]

SPDEF (Sam pointed domain containing ETS transcription factor) is a prostate-derived ETS factor that maintains homeostasis and differentiation of epithelial tissues and heritable alterations in cancer. SPDEF gene is important for normal cell growth, development, survival and function. Previous studies have suggested a possible oncogenic function of SPDEF[39].

It has been found that SPDEF is down-regulated in invasive breast cancer cell lines which is supportive of its role in tumor suppression[27,52]. Depending on the molecular subtype of the disease, SPDEF has a different role in breast cancer.

Overexpression of SPDEF mRNA is associated with poor overall survival in estrogen receptor positive breast cancer. Similar to this, the reduction of SPDEF in several luminal cell lines reduced proliferation and enhanced basal apoptosis[16]. Owing to its potential role in breast cancer

etiology and progression, SPDEF could be a potential target for cancer diagnosis and therapeutics[61].

Natural substances such as plant-derived chemicals demonstrated notable anti-breast cancer characteristics among medications that can be created to treat the disease. These compounds are classified as flavonoids, terpenoids and alkaloids, among other chemical groups. Phytoconstituents show anti-carcinogenic actions mediated by a number of different molecular mechanisms including the suppression of extrinsic and intrinsic apoptotic pathways, the arrest of the cell cycle and the activation of autophagy, to carry out their cytotoxic actions against breast cancer cell lines both *in vitro* and *in vivo*. In addition to their direct effects on cancer cells, phytoconstituents also influence certain aspects of angiogenesis such as endothelial cell development and sprouting, the production of micro-capillary tubes and the suppression of a number of cell signalling pathways.

Additionally, only particular medicines were associated with the chemoprevention effects of these bioactive substances[32]. Breast cancer has been proven to be inhibited and the increased lipid levels have been shown to be healed by phytoconstituents. Breast cancer drugs target the ER (estrogen receptor alpha), PR (progesterone receptor), EGFR (epidermal growth factor receptor) and other receptors. PR overexpression is commonly seen in breast cancer cell lines[3]. A number of studies have shown several phytoconstituents as potential drugs against different kinds of cancers[31]. Considering the importance of phytoconstituents as drug agents against cancer and the role of SPDEF in breast cancer, computer-aided drug design (CADD) approach was utilized to identify potential drug agents against SPDEF protein.

In the current study, pharmacokinetic properties like absorption, distribution, metabolism, excretion and toxicity (ADMET), drug-likeness, bioactivity score and molecular docking analysis were performed using *in silico* approaches. For this study, SwissADME, ProTox II, Molsoft, molinspiration, PyRx and Biovia Discovery Studio were used. A total of fifteen phytoconstituents belonging to diverse classes were assessed for their pharmacokinetic properties, targeting the SPDEF protein.

Material and Methods

Plant-based phytoconstituents: Fifteen phytoconstituents were selected based on their role in cancer therapeutics as shown in literature[1,5,7,18,20,26,35-37,49,57,58,60,62]. These are silibinin, codonolactone, genistein, 2-hydroxychalcone, baicalein, calycosin, fisetin, 2-methylanthraquinone, curcumin, icaritin, noscapine, scopoletin, catechol, ajoene and allicin. The class, source, molecular formula and PubChem ID of the selected phytoconstituents are given in table 1. The Simplified Molecular Input Line Entry System (SMILES) notation of each phytoconstituent was downloaded from PubChem. The two-dimensional structure of each phytoconstituent was designed in ChemSketch using the respective SMILES notation of each individual compound (Fig. 1).

Predictions of pharmacokinetics, physicochemical property, drug-likeness and toxicity of selected phytoconstituents: For pharmacokinetics, physicochemical properties like drug likeness and toxicity analyses, the SMILES format of the phytoconstituents were used. ADMET structure-activity relationship was performed by the SwissADME web tool (http://www.swissadme.ch)[24]. SMILES notations were also used to examine drug-likeness and the ADME profiles. The drug likeliness of all the ligands was evaluated using Lipinski's rule of five to see if all the attributes were within the acceptable range. The partition coefficient (Log P) was used to examine the lipophilicity levels of the phytoconstituents. Pharmacokinetics properties {Gastrointestinal (GI) absorption, skin permeability (Log Kp), P-glycoprotein substrate and blood-brain barrier (BBB) permeation} were examined to determine absorption and distribution of the phytoconstituents within the body. The CYP inhibition parameters (CYP1A2, CYP2C19, CYP2C9, CYP2D6 and CYP3A4) were used to estimate the phytoconstituent metabolism.

For their identification as a viable therapeutic candidate, all the significant ADMET parameters of the phytoconstituents were thoroughly estimated and confirmed for compliance with their standard ranges. In terms of bioavailability, drug-likeness evaluates qualitatively the likelihood that a molecule would be used as an oral drug. Drug likenesses were obtained from Molsoft (http://www.molsoft.com/mprop/). The Molinspiration website was used to predict the bioactivity score of the phytoconstituents[38]. The overall procedure from the retrieval of phytoconstituents to their screening by different tools is given as a flow chart (Fig. 2).

The toxicological endpoints (hepatotoxicity, carcinogenicity, immunotoxicity, mutagenicity and cytotoxicity) and acute toxicity class (LD50, mg/Kg) of the selected fifteen phytoconstituents were calculated on the ProTox-II server[12].

Preparation of the target proteins and ligands for docking studies: The PubChem database (https://pubchem.ncbi.nlm.nih.gov/) was searched for the 3D structures of ligands. The ligand structures in .sdf files (structure dimension files) were optimized and converted to PDB file (protein data bank file) using PyMol software (https://pymol.org/2/). The X-ray crystal structure of the targeted protein SPDEF (PDB ID: 2DKX) was retrieved as a pdb file from the Protein Data Bank (https://www.rcsb.org/) for docking[17]. The molecular docking was carried out using PyRx software. PyRx is written in the Python programming language and is compatible with virtually all the current computers. Molecular docking simulation is one such computer tool that can be used to assess the quality of an interaction between a

ligand and its protein target. Molecular docking was performed using PyRx V 0.8 virtual screening software[51].

After customizing the docking settings, the .pdb files of the protein and ligands interactions were produced and saved. To evaluate the effectiveness of the molecular docking, we looked at how well different ligands bind to the target at zero RMSD (Root Mean Square Deviation). The molecular interaction within the binding pocket of the target proteins was then visualized using Biovia Discovery Studio Visualizer for the best-docked complexes. The binding energy values were graphed using MS Excel.

Representation of the binding pockets: The best docking orientations were subsequently analyzed using Accelrys Biovia Discovery Studio version 2022[47]. The Biovia Discovery Studio was used to upload the PyRx data (Dimension log file converted into PDB). Run Analysis option was chosen and the protein-ligand docked structure was viewed in three dimensions. When a protein and ligand combination is submitted, Biovia Discovery Studio produces several distinct interactions between the protein and ligand that stabilize the system. The binding pockets of the ligand were again re-verified using a free academic edition of PyMOL (https://pymol.org/2/)[25] in addition to visualization by Biovia Discovery Studio.

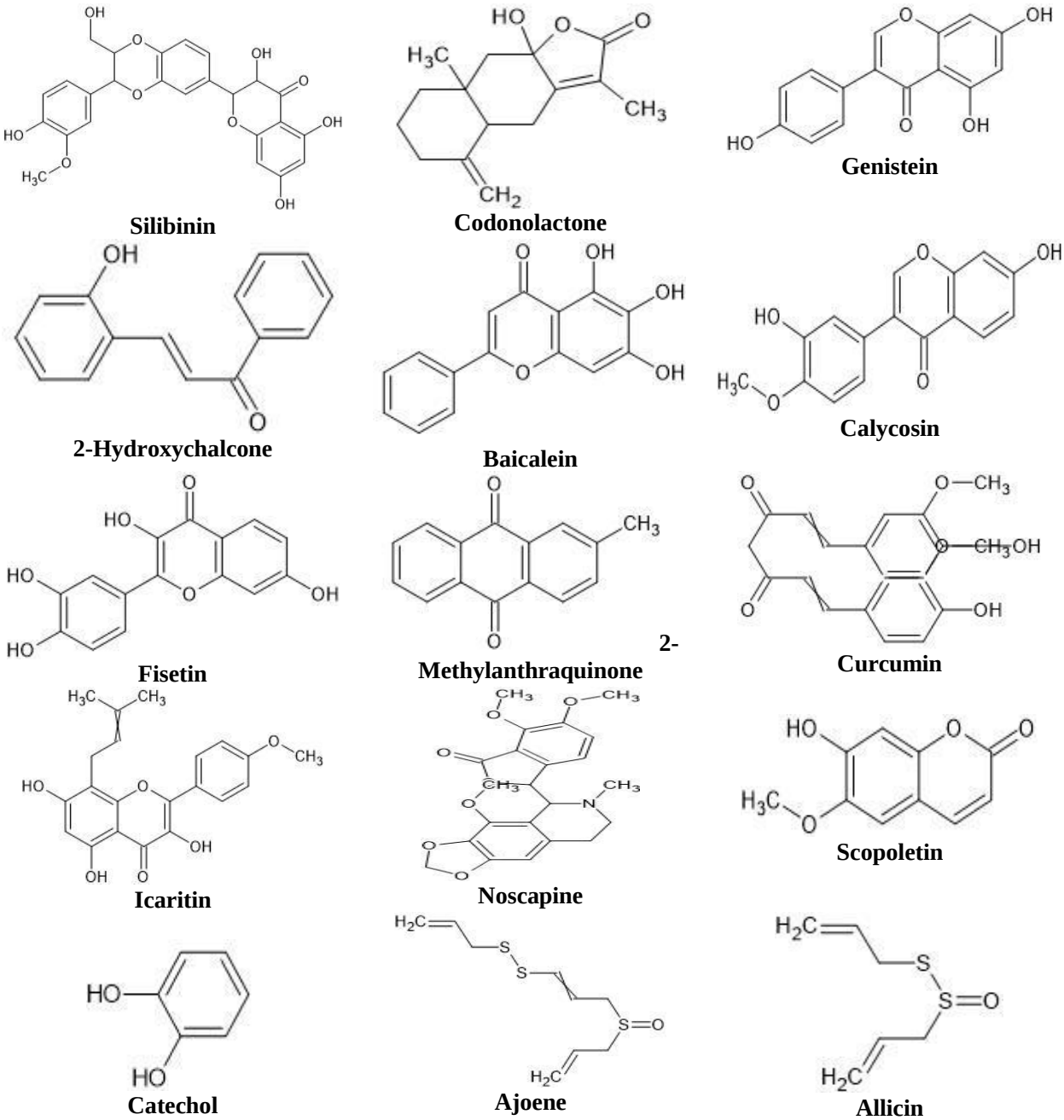

Fig. 1: Chemical structure of phytoconstituents from different plant species retrieved from PubChem and designed in ChemSketch. The SMILES notation of each phytoconstituent, downloaded from PubChem, was input into Chemsketch to draw its two-dimensional (2D) structure. Each 2D structure was exported in JPEG format and represented in this figure.

Table 1
Details of the selected phytoconstituents from different plants retrieved from PubChem. The PubChem ID and molecular formula were downloaded from PubChem

S.N.	Phytoconstituent	Type of compound (Class)	Source of Phytoconstituent	PubChem ID	Molecular formula
1	Silibinin	Metabolites (Polyphenolic flavonoid)	*Silybum marianum*	31553	$C_{25}H_{22}O_{10}$
2	Codonolactone	Metabolites (Sesquiterpene lactone)	*Chloranthus henryi Hemsl*	155948	$C_{15}H_{20}O_3$
3	Genistein	Secondary metabolites (Isoflavones)	*Garcinia indica*	5280961	$C_{15}H_{10}O_5$
4	2-Hydroxychalcone	Secondary metabolites (Chalcones)	*Cryptocarya concinna*	5367146	$C_{15}H_{12}O_2$
5	Baicalein	Secondary metabolites (Flavones)	*Scutellaria baicalensis*	5281605	$C_{15}H_{10}O_5$
6	Calycosin	Metabolites (7-hydroxyisoflavones)	*Astragalus membranaceus*	5280448	$C_{16}H_{12}O_5$
7	Fisetin	Secondary metabolites (Flavonoid)	*Fragaria ananassa*	5281614	$C_{15}H_{10}O_6$
8	2-Methylanthraquinone	Secondary metabolites (Anthraquinone)	*Clausena heptaphylla*	6773	$C_{15}H_{10}O_2$
9	Curcumin	Metabolites (Curcuminoids)	*Curcuma longa*	969516	$C_{21}H_{20}O_6$
10	Icaritin	Secondary metabolites (8-prenylated flavones)	*Epimedium rubrum*	5318980	$C_{21}H_{20}O_6$
11	Noscapine	Secondary metabolites (Benzylisoquinoline alkaloid)	*Papaver somniferum*	275196	$C_{22}H_{23}NO_7$
12	Scopoletin	Metabolites (7-hydroxycoumarins)	*Sinomonium acutum*	5280460	$C_{10}H_8O_4$
13	Catechol	Metabolites (Phenolic)	*Allium cepa*	289	$C_6H_6O_2$
14	Ajoene	Secondary metabolites (organosulfur compound)	*Allium sativum*	5386591	$C_9H_{14}OS_3$
15	Allicin	Secondary metabolites (Organosulfur compound)	*Allium sativum*	65036	$C_6H_{10}OS_2$

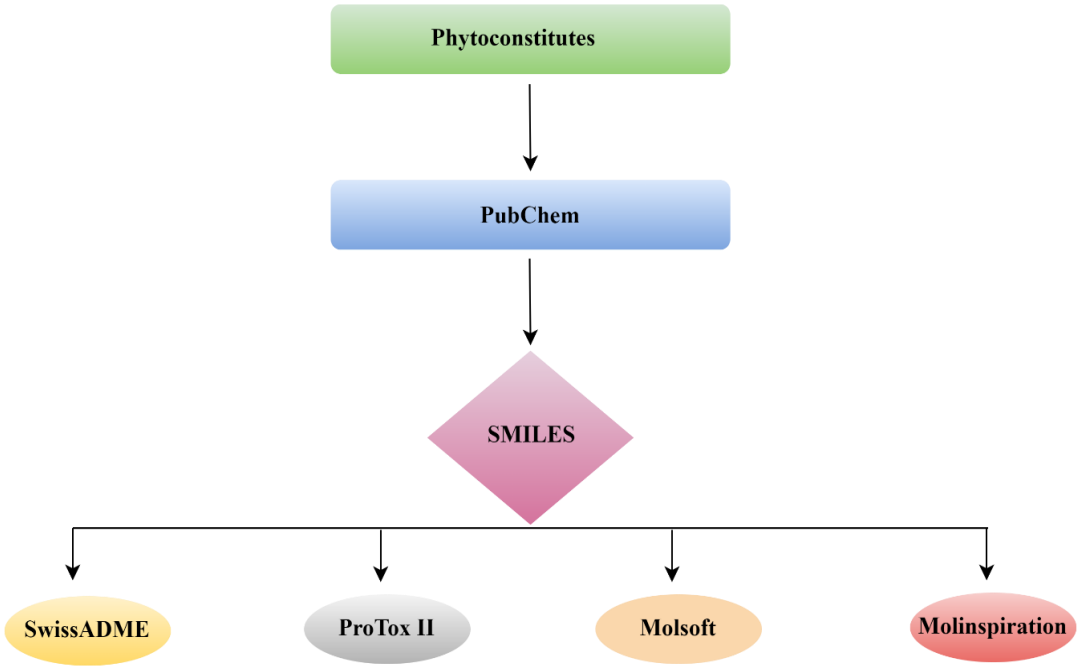

Fig. 2: Schematic representation of the ADMET analysis of the phytoconstituents. The SMILES notation for each compound was retrieved from PubChem and subjected to ADMET analysis using different bioinformatics tools.

Molecular dynamics and Simulations: The behavior of protein-ligand complex structures at the atomic level is studied computationally using molecular dynamics simulations[8]. Using GROMACS version 2021.3 package[2,13], the MD simulation analysis was executed with the parameters and topology was initiated with CHARMm36-jul2022[40]. With CHARMm-GUI compatibility, the top three docked (protein-ligand) structure topology files were developed[55]. The most recent CHARMM Swiss Param server was used to prepare the top three docked chemical compounds[64]. The cubic box type was applied to solvate the structure and SPC water models that extended 10 Å from the protein, were used. Na^+ ions with a physiological salt concentration of 9 were added to the system. The steepest descent strategy with 5000 steps was used for energy minimization. In order to achieve equilibration, 300K and 1.0bar pressure were the NPT (constant number of particles, pressure and temperature) and NVT (constant number of particles, volume and temperature) conditions.

200 ns of simulation time were used in the production run with the Leap-frog MD integrator[6]. For the stability and compactness of the protein complex structure, graphs representing root mean square deviation (RMSD), root mean square fluctuation (RMSF), solvent accessible surface area (SASA) and radius of gyration (RoG) were computed. The total number of hydrogen interactions between the protein and ligand structure is displayed in H-bond graphs. Plots were developed with Grace Software while simulations were produced using NVIDIA Tesla V100 GPU cards and Intel Xeon Cascade Lake CPUs at IIT Gandhinagar's PARAM-ANANTA HPC facility. 7400 CPU cores and 52TB of RAM.

Results and Discussion

Prediction and analysis of the physicochemical properties of phytoconstituents by using SwissADME tool: According to Christopher Lipinski et al[34], the properties of the ligand molecules like molecular mass (g/mol) ≤ 500, calculated octanol/water partition coefficient (cLogP) ≤ 5, number of hydrogen bond donors (nOHNH) ≤ 5, number of hydrogen bond acceptors (nON) ≤ 10 should be in this range. According to the "rule of five", the compounds with characteristics that deviated from above-mentioned boundaries would be less likely to be orally absorbed. In the present study, all the phytoconstituents obeyed Lipinski's rule of five for oral availability.

Table 2
The physicochemical properties of phytoconstituents. The SMILES notation for each compound was retrieved from PubChem and subjected to ADME analysis using SwissADME tool.

S. N.	Phytoconstituent	Molecular weight (g/mol)	% Absorptino (>50%)	(TPSA) (Å)^2 (<140)	Heavy atom count (n atoms)	H-bond donors (nOHNH) (≤5)	H-bond acceptors (nON) (≤10)	No. of rotatable bonds (≤10)	logS	cLogP
1	Silibinin	482.4	55.477	155.14	35	5	10	4	-4.14	2.79
2	Codonolactone	248.32	62.47	46.53	18	1	3	0	-2.70	2.46
3	Genistein	270.24	77.64	90.9	20	3	5	1	-3.72	1.91
4	2-Hydroxych alcone	224.25	96.1315	37.3	17	1	2	3	-3.98	2.19
5	Baicalein	270.24	77.64	90.9	20	3	5	1	-4.03	2.43
6	Calycosin	284.26	81.435	79.9	21	2	5	2	-3.57	2.40
7	Fisetin	286.24	70.661	111.13	21	4	6	1	-6.44	1.50
8	2 Methylanthraquinone	222.24	97.222	34.14	17	0	2	0	-4.22	2.20
9	Curcumin	368.4	76.895	93.06	27	2	6	8	-3.94	3.27
10	Icaritin	368.4	74.456	100.13	27	3	6	4	-5.30	3.21
11	Noscapine	413.4	82.887	75.69	30	0	8	4	-4.14	3.29
12	Scopoletin	192.17	88.414	59.67	14	1	4	1	-2.46	1.86
13	Catechol	110.11	95.042	40.46	8	2	2	0	-1.63	1.13
14	Ajoene	234.4	79.027	86.88	13	0	1	8	-1.84	2.74
15	Allicin	162.27	87.755	61.58	9	0	1	5	-1.34	1.95

*Percentage absorption was calculated as: % absorption = 109 − [0.345 × Topological Polar Surface Area].
Topological polar surface area (defined as a sum of surfaces of polar atoms in a molecule)

Lipinski's rule of five is essential to follow for rational drug design and it has been proposed that when one of Lipinski's rules of five is disobeyed, a given molecule will likely to have low permeability or poor absorption. The surface sum of overall polar atoms, predominantly oxygen and nitrogen, as well as their connected hydrogen atoms, is referred to as a molecule's topological polar surface area (TPSA). It was observed that molecules with identical molecular masses (baicalein and genistein; 2-hydroxychalcone and 2-methylanthraquinone) had similar TPSA and % absorption values (Table 2) while molecules with a TPSA of 60 $Å^2$ would be efficiently absorbed (> 90% fractional absorption) and those with a TPSA of 140 $Å^2$ and beyond would be poorly absorbed (<10% fractional absorption)[22].

All phytoconstituents showed good intestinal absorption except silibinin (155.14 $Å^2$). 2-methylanthraquinone has the highest percent absorption (97.222%) among the fifteen investigated phytoconstituents, according to an examination of the % Abs.

ADMET analysis was done to understand the pharmacokinetic characteristics. An essential characteristic of a drug-like molecule is solubility, given as log S, which is defined as the 10-based logarithm of a molecule's solubility measured in mol/L. It is directly related to a drug's water solubility, with optimal values ranging from -6.5 and 0.5[30]. All the phytoconstituents follow this range. Fisetin (-6.44) is the least soluble molecule and allicin (-1.34) has the highest solubility, according to the calculated result of log S tabulated in table 2. Any single bond that is not in a ring and is attached to a nonterminal heavy (non-hydrogen) atom is said to be rotatable. A key factor in influencing a drug's oral bioavailability is the number of rotatable bonds, which measures molecular flexibility[56]. The molecule should not have more than 9 rotatable bonds[30]. In our study, the number of rotatable bonds ranged from 1-8, some phytoconstituents like codonolactone, 2-methylanthraquinone and catechol have not possessed any rotatable bonds (Table 2).

Drug-likeness and ADME prediction of the phytoconstituents by using SwissADME and Molinspiration tools: The blood-brain barrier, a special property of the blood arteries that vascularize the central nervous system (CNS), enables these vessels to tightly control the transport of ions, chemicals and cells between the blood and the brain[15].

To study the distribution of the phytoconstituents across Blood Brain Barrier (BBB), permeability parameters were considered. Using the SwissADME web tool, we predicted that codonolactone, 2-hydroxychalcone, 2-methylanthraquinone, scopoletin, catechol, allicin can permeate BBB, but silibinin, genistein, baicalein, calycosin, fisetin, icaritin, noscapine, scopoletin and ajoene cannot permeate BBB (Table 3).

Table 3
The SMILES notation of each compound has been used for interaction of target phytoconstituents with cytochromes P450 isoforms predicted using SwissADME and drug-likeness by using Molsoft.

S.N.	Phytoconstituent	Drug score	Lipophilicity (Log Po/w)	BBB permeant	P- gp substrate	CYP1A2 Inhibitor	CYP2C19 Inhibitor	CYP2C9 Inhibitor	CYP2D6 Inhibitor	CYP3A4 Inhibitor	Log Kp (cm/s)	Lipinski's violation	GI Absorption
1	Silibinin	0.84	2.79	No	No	No	No	No	No	Yes	-7.89	0	Low
2	Codonolactone	-0.38	2.34	Yes	No	No	No	No	No	No	-6.32	0	High
3	Genistein	0.44	1.91	No	No	Yes	No	No	Yes	Yes	-6.05	0	High
4	2-Hydroxych alcone	-0.84	2.19	Yes	No	No	Yes	Yes	No	No	-4.93	0	High
5	Baicalein	-0.1	2.43	No	No	Yes	No	No	Yes	Yes	-5.7	0	High
6	Calycosin	0.16	2.4	No	No	Yes	No	No	Yes	Yes	-6.3	0	High
7	Fisetin	0.46	1.5	No	No	Yes	No	No	Yes	Yes	-6.65	0	High
8	2-Methylan thraquinone	-0.69	2.2	Yes	No	Yes	Yes	No	No	No	-4.86	0	High
9	Curcumin	-0.82	3.27	No	No	No	No	Yes	No	Yes	-6.28	0	High
10	Icaritin	0.84	3.21	No	No	No	No	Yes	No	No	-5.16	0	High
11	Noscapine	0.54	3.29	No	No	No	Yes	Yes	Yes	Yes	-6.9	0	High
12	Scopoletin	-1.23	1.86	Yes	No	Yes	No	No	No	No	-6.39	0	High
13	Catechol	-1.44	1.13	Yes	No	No	No	No	No	Yes	-6.35	0	High
14	Ajoene	-1.01	2.74	No	No	No	No	Yes	No	No	-6.52	0	High
15	Allicin	-0.84	1.95	Yes	No	No	No	No	No	No	-6.36	0	High

* logKp skin permeation, GI = gastrointestinal, BBB = blood brain barrier

The rate at which a substance permeates the stratum corneum is determined by the skin permeability (Log Kp). This number is frequently used to quantify the movement of molecules in the epidermal skin's outermost layer and highlights the importance of skin absorption[19]. It is found that log Kp decreases (less negative) with the increase in molecular size. The skin permeability (Log Kp) values for all of the phytoconstituents ranged from -7.89 to -2.67 cm/s indicating low skin permeability[38].

Although there have been some studies looking at the possibility of stereo selectivity in the action of the permeability glycoprotein (P-gp), this key protein transporter is involved in the disposition of many medicines with various chemical structures[21]. Because of the reduced clearance and accumulation of the drug or its metabolites, this could result in pharmacokinetics-related drug-drug interactions that could have toxic or other undesirable side effects[29].

The most significant enzyme system for phase 1 metabolism of medications or pharmaceuticals such as herbal treatments and environmentally harmful substances, is the cytochrome P450 (CYP) enzyme family. One of the main mechanisms producing pharmacokinetic drug-drug interactions is the inhibition and activation of CYPs[28]. It was found that genistein, baicalein, calycosin, 2-methylanthraquinone and curcumin are the molecules that can act as CYP1A2 (Cytochrome P450 Family 1 Subfamily A Member 2) inhibitors whereas silibinin, codonolactone, 2-hydroxychalcone, icaritin, noscapine, scopoletin, catechol ajoene and allicin cannot act as CYP1A2 inhibitors (Table 3).

The phytoconstituents evaluated in this investigation, except silibinin, genistein, baicalein, calycosin, fisetin, noscapine, scopoletin and catechol are expected to interact with CYP3A (Cytochrome P450, family 3, subfamily A), making them very suitable molecules as CYP3A4 probes. The therapeutic effectiveness and toxicity of many medications are significantly influenced by CYP3A4 enzymes[54].

Genistein, baicalein, calycosin, fisetin and noscapine are predicted as CYP2D6 (Cytochrome P450 2D6) inhibitors whereas silibinin, codonolactone, genistein, baicalein, calycosin, fisetin, curcumin, icaritin, scopoletin, catechol, ajoene and allicin cannot act as CYP2D6 inhibitors (Table 3).

2-hydroxychalcone, 2-methylanthraquinone and noscapine can act as CYP2C19 (cytochrome P450 family 2 subfamily C member 19) inhibitor. 2-hydroxychalcone, icaritin, noscapine, scopoletin and ajoene can act as CYP2C9 (Cytochrome P450 family 2 subfamily C member 9) inhibitor whereas silibinin, codonolactone, genistein, baicalein, calycosin, fisetin, 2-methylanthraquinone, curcumin, catechol and allicin cannot act as CYP2C9 inhibitor. According to a previous analysis, the CYP enzymes' induction and inhibition are most likely the common causes of drug interactions[28].

The GI absorption of orally administered drugs is determined by not only the absorptivity of GI mucosa, but also by the transportation rate in the GI tract[50]. All the fifteen phytoconstituents showed high GI absorption except silibinin.

The traditional definition of lipophilicity is the partition coefficient of n-octanol and water (log Po/w). Due to the vital significance of this physicochemical property for pharmacokinetics drug discovery, it has a distinct area in SwissADME[11]. A molecule with a drug-likeness score of more than 0.00 is most likely to exhibit significant biological activity whereas values -0.50 to 0.00 are predicted to be moderately active and a score less than -0.50 is presumed to be inactive[9]. The magnitude of drug-likeness score of the phytoconstituents ranged from -1.44 to 0.89 according to the analysis done in molsoft tool. Silibinin (0.84), genistein (0.44), calycosin (0.16), fisetin (0.46), icaritin (0.84) and noscapine (0.54) were predicted to be significantly active; codonolactone (-0.38), baicalein (-0.1), scopoletin (-1.23), catechol (-1.44) and allicin (-1.01) were predicted to be moderately active; 2-Hydroxychalcone (-0.8), 2 Methylanthraquinone (-0.69), curcumin (-0.82) and allicin (-0.84) were predicted to be incative.

Predition of toxicity profile of the fifteen phytoconstituents by using ProTox tool: One of the main considerations while choosing a molecule as a potential therapeutic candidate is the absence of toxicity[45]. The toxicological endpoints (carcinogenicity, immunotoxicity, mutagenicity and cytotoxicity) and the organ toxicity (hepatotoxicity) of the fifteen phytoconstituents were predicted in the current study. Their qualitative assessment was performed based on binary (active or inactive for certain cell types), cytotoxicity, immunotoxicity and hepatotoxicity parameters. The quantitative assessment was done on the basis of LD50 (lethal dose) values[43].

Using Pro Tox II, several of the toxicity metrics such as hepatotoxicity, carcinogenicity, immunotoxicity, mutagenicity, cytotoxicity, LD50 values and acute toxicity class, were calculated[14]. The toxicological endpoints, organ toxicity, LD50 score and acute toxicity class have been explained in table 4. The results demonstrate that none of the phytoconstituents is hepatotoxic. The results also showed that all of the phytoconstituents are not cytotoxic except noscapine and all of the phytoconstituents are not mutagenic except 2-methylanthraquinone and baicalein. Of the considered phytoconstituents, scopoletin showed two toxicological endpoints i.e. carcinogenicity and immunotoxicity and baicalein showed carcinogenicity and mutagenicity (Table 4).

On the other hand, genistein, allicin, 2-hydroxychalcone and ajoene were free from any of the predicted toxicological

endpoints. Acute toxicity predictions showed that the phytoconstituents considered are not fatal; however, they can be classified as detrimental toxic classes. The results for the median lethal dose (LD50) were observed to be between 100 and 3919 mg/Kg.

Table 4
The SMILES notation of each compound has been used for organ toxicity, toxicological endpoints and acute toxicity prediction via Pro Tox II tool.

S. N.	Phytoconstituents	Hepatotoxicity	Carcinogenicity	Immunotoxicity	Mutagenicity	Cytotoxicity	LD_{50}(mg/Kg)	Acute Toxicity class
1	Silibinin	Inactive	Inactive	Active	Inactive	Inactive	2000	4
2	Codonolactone	Inactive	Inactive	Active	Inactive	Inactive	2000	4
3	Genistein	Inactive	Inactive	Inactive	Inactive	Inactive	2500	5
4	2-Hydroxychalcone	Inactive	Inactive	Inactive	Inactive	Inactive	1048	4
5	Baicalein	Inactive	Active	Inactive	Active	Inactive	3919	5
6	Calycosin	Inactive	Inactive	Active	Inactive	Inactive	2500	5
7	Fisetin	Inactive	Active	Inactive	Inactive	Inactive	159	3
8	2-Methylanthraquinone	Inactive	Inactive	Inactive	Active	Inactive	2795	5
9	Curcumin	Inactive	Inactive	Active	Inactive	Inactive	2000	4
10	Icaritin	Inactive	Inactive	Active	Inactive	Inactive	3919	5
11	Noscapine	Inactive	Active	Active	Inactive	Active	840	4
12	Scopoletin	Inactive	Active	Active	Inactive	Inactive	3800	5
13	Catechol	Inactive	Active	Inactive	Inactive	Inactive	100	3
14	Ajoene	Inactive	Inactive	Inactive	Inactive	Inactive	1600	4
15	Allicin	Inactive	Inactive	Inactive	Inactive	Inactive	874	4

Table 5
Bioactivity Scores of selected phytoconstituents by using Molinspiration tool by using SMILES notation of each compound

S. N.	Phytoconstituents	GPCR ligand	Ion channel modulator	Kinase inhibitor	Nuclear receptor ligand	Protease inhibitor	Enzyme inhibitor
1	Silibinin	0.07	-0.05	0.01	0.16	0.02	0.23
2	Codonolactone	-0.13	0.28	-0.65	0.36	-0.33	0.58
3	Genistein	-0.22	-0.54	-0.06	0.23	-0.68	0.13
4	2-Hydroxychalcone	-0.34	-0.17	-0.54	-0.3	-0.51	-0.05
5	Baicalein	-0.12	-0.18	0.19	0.17	0.35	0.26
6	Calycosin	-0.25	-0.65	-0.08	0.06	-0.78	0.01
7	Fisetin	-0.11	-0.27	0.18	0.2	-0.36	0.2
8	2-Methylanthraquinone	-0.37	-0.25	-0.29	-0.38	-0.49	-0.07
9	Curcumin	-0.06	-0.2	-0.26	0.12	-0.14	0.08
10	Icaritin	-0.03	-0.32	0.08	0.49	-0.26	0.32
11	Noscapine	-0.04	-0.02	-0.51	-0.45	-0.45	-0.12
12	Scopoletin	-1	-0.65	-0.95	-0.81	-1.16	-0.24
13	Catechol	-3.04	-2.51	-3.1	-2.98	-3.24	-2.67
14	Ajoene	-0.67	-0.99	-1.32	-0.73	-0.63	0.24
15	Allicin	-2.51	-2.26	-2.95	-2.66	-1.4	-1.52

As per the globally harmonized system of classification of labeling of chemicals (as described in Pro Tox II), fisetin and catechol were predicted as toxic (Class III); allicin, 2-hydroxychalcone, silibinin and codonolactone were harmful (Class IV) and the rest were categorized into "may be harmful" (Class V and class VI) toxicity classes. The results indicated that all the phytoconstituents could not be hepatotoxic.

Bioactivity score (BAS) prediction: A drug candidate should not only strongly bind to the target, but also produce the necessary bioactivity. The BAS score for the selected phytoconstituents was calculated using a web-based program called Molinspiration. The six primary pharmacological targets used in computational drug discovery are G-protein coupled receptors (GPCRs), ion channels, kinases, nuclear receptors, protease and enzymes. To assess the drug's effectiveness and mode of action, bioactivity is measured. More than 0.00 is seen as active, -5.0 and 0.0 are regarded as somewhat active and less than -5.0 is regarded as inactive[59]. As an enzyme inhibitor, silibinin, codonolactone, genistein, baicalein, calycosin, fisetin, curcumin, icaritin and ajoene showed the greatest bioactivity.

For bioactivity, G-protein coupled receptors (GPCRs) ligand, ion channels modulator, kinases, nuclear receptors, protease and enzymes inhibition prediction values for 2-hydroxychalcone, 2-methylanthraquinone, noscapine, scopoletin, catechol and allicin are less than 0.00. GPCR ligand prediction values for silibinin are greater than 0.00. Ion channels modulator prediction values for codonolactone are greater than 0.00. Nuclear receptor ligand prediction values for silibinin, codonolactone, genistein, baicalein, calycosin, fisetin, curcumin and icaritin are greater than 0.00. Protease inhibition prediction values for silibinin and baicalein are greater than 0.00. Enzyme inhibition prediction values for silibinin, codonolactone, genistein, baicalein, calycosin, fisetin, curcumin, icaritin and ajoene are greater than 0.00. There was no phytoconstituent with the bioactivity prediction value less than -5.00 (Table 5).

Silibinin, Codonolactone and Genistein acting as potential anticancer phytoconstituents against SPDEF: Presently, it is of great interest to create inhibitors for the breast cancer target SPDEF by performing virtual screening and molecular docking using plant-based compounds. Using the same approach, different cancer-related targets like NUDT5 (nucleotide diphosphate hydrolase type 5)[48], APC10/DOC1 (Anaphase-Promoting Complex subunit 10/Death of Cyclase 1) and PKM2 (Pyruvate kinase Muscle isozyme M2)[42], estrogen receptor alpha, progesterone receptor and EGFR (epidermal growth factor receptor)[44] have been used for molecular docking study against various natural compounds like 7-[[5-(3,4-dichlorophenyl)-1,3,4-oxadiazol-2-yl]methyl]-1,3-dimethyl-8-piperazin-1-yl-purine-2,6-dione, 8-oxo-2'-deoxy-guanosine-5'-monophosphate, Alpha-beta methylene ADP-ribose, Adenosine monophosphate, Resveratrol, Mitomycin-C, Colchicine, Paclitaxel, Shikonin, Cholesterol margarate, 7-Dehydrodiosgenin, Stigmastan-3,5-diene and γ-Sitosterol.

However, there is a lack of information related to the molecular docking study of SPDEF protein as a target with phytoconstituents. In the current study, SPDEF has been used as a potential target protein as it plays a significant role in tumor suppression. Fifteen phytoconstituents were selected based on their medicinal importance.

A molecular docking study was carried out to determine the binding affinities, binding types and active amino acid residues of studied compounds in the target enzyme.

Table 6
The binding energies in .csv file format obtained by using the .pdb files of individual protein-ligand complexes generated in PyRx.

S.N.	Phytoconstituents	Binding Energy (kcal/mol)
1	Silibinin	-7.7
2	Codonolactone	-6.1
3	Genistein	-6.1
4	2-Hydroxychalcone	-6
5	Baicalein	-6
6	Calycosin	-6
7	Fisetin	-6
8	2-Methylanthraquinone	-5.9
9	Curcumin	-5.8
10	Icaritin	-5.8
11	Noscapine	-5.7
12	Scopoletin	-5.2
13	Catechol	-4.1
14	Ajoene	-3.7
15	Allicin	-3.5

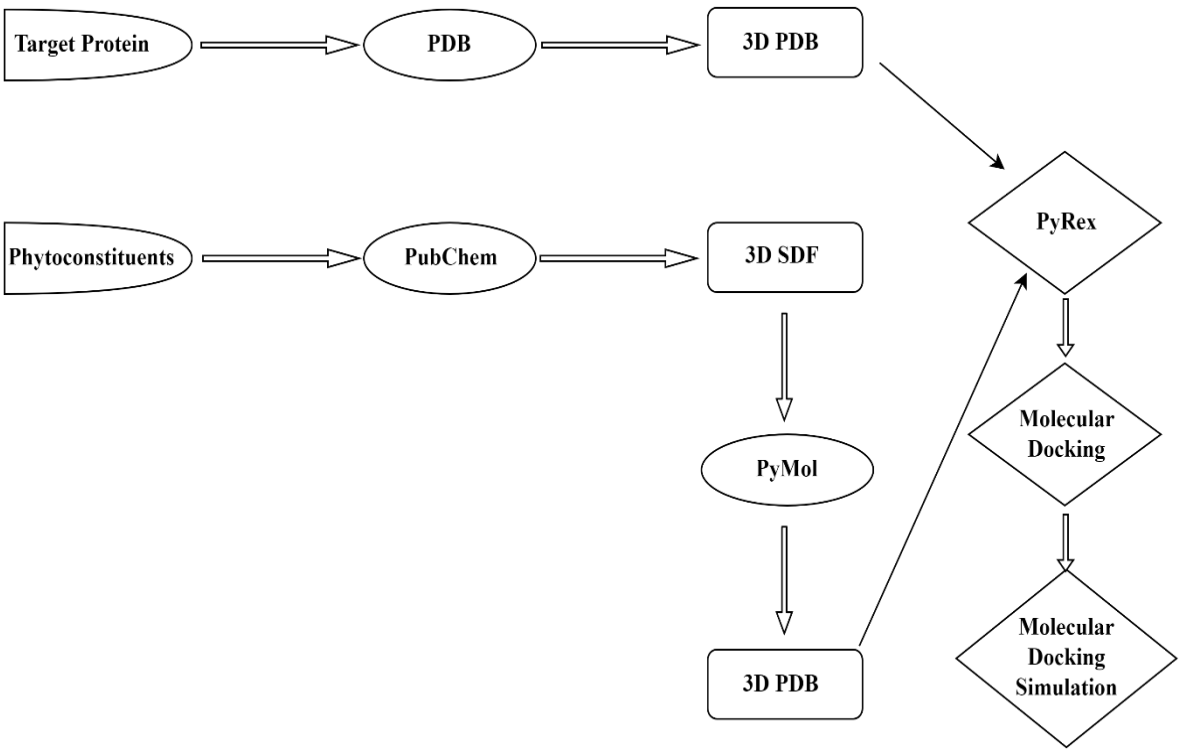

Fig. 3: Schematic representation of protein-ligands molecular docking and molecular dynamic simulation analysis flowchart

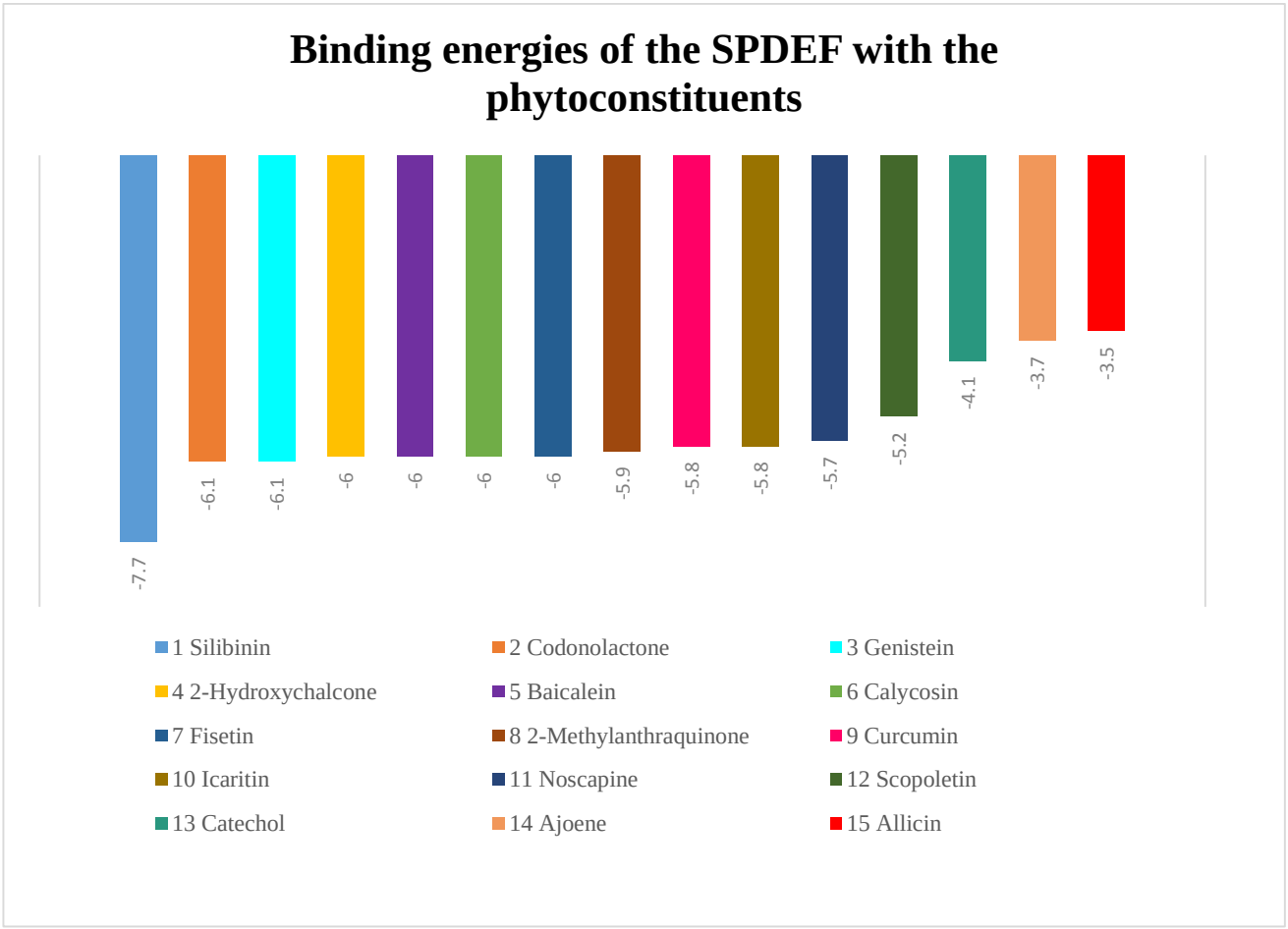

Fig. 4: Graphical representation of the binding energies of the selected fifteen phytoconstituents with SPDEF. These values were obtained by uploading the .pdb files of SPDEF and the phytoconstituents into PyRx software.

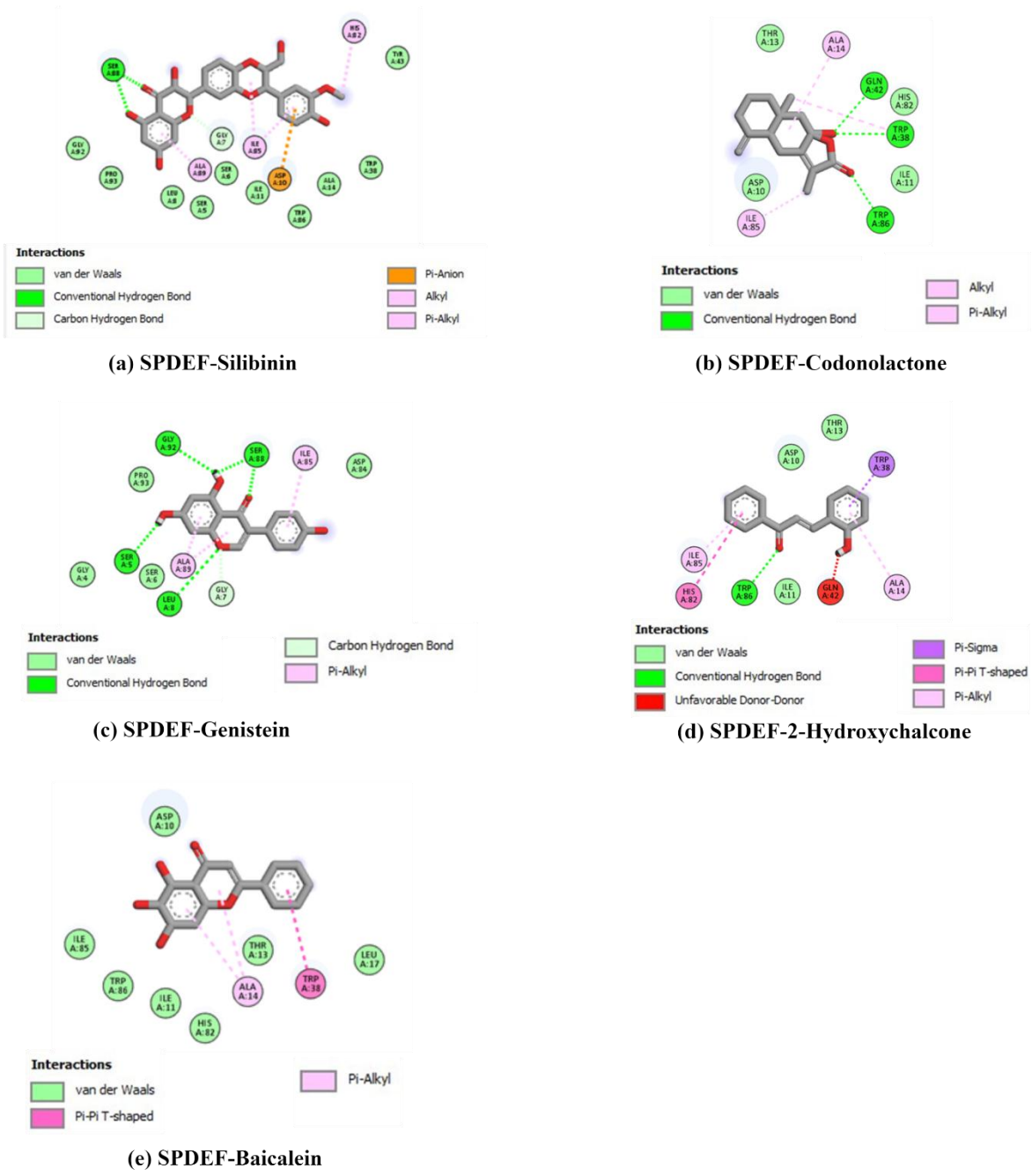

Fig. 5: Schematic 2-D representations of SPDEF-phytoconstituents complexes, generated using Biovia Discovery Studio. Only the best five complexes, based on binding energy values, are represented here. The alphabets a-e stand for (a) SPDEF-Silibinin, (b) SPDEF-Codonolactone, (c) SPDEF-Genistein, (d) SPDEF-2-Hydroxychalcone and (e) SPDEF-Baicalein. These figures were produced by using the .pdb files of individual protein-ligand complexes generated in PyRx. The .pdb files were uploaded into Biovia Discovery Studio software.

The goal of the study was to predict the binding affinity of fifteen selected phytoconstituents to the target protein i.e. SPDEF. The studied phytoconstituents displayed binding energies ranging from -7.7 to -3.5 kcal/mol which have been summarized in table 6. These were the binding energies of silibinin (-7.7), codonolactone (-6.1), genistein (-6.1), 2-hydroxychalcone (-6), baicalein (-6), calycosin (-6), fisetin (-6), 2-methylanthraquinone (-5.9), curcumin (-5.8), icaritin (-5.8), noscapine (-5.7), scopoletin (-5.2), catechol (-4.1), ajoene (-3.7) and allicin (-3.5) towards target protein SPDEF. The negative binding energies of the phytoconstituents with SPDEF are graphed separately (Fig. 4).

The top three phytoconstituents with low binding energies were silibinin, codonolactone and genistein. *In silico* docking analysis indicated that silibinin interacts with the SPDEF residues at SER-5, ASP-10, SER-88, ILE-11 and ALA-89 with binding energy -7.7 kcal/mol. It was found that codonolactone interacts with the SPDEF residues at TRP-38,

GLN-42, HIS-82, TRP-86, ASP-10, THR-13, ALA-14 and -HIS-82 with binding energy -6.1 kcal/mol. For genistein, it was reported that it interacts with SPDEF residues at SER-5, SER-88, LEU-8, ILE-85 and ALA-89 with binding energy -6.1 kcal/mol. The binding energy data indicate that these three phytoconstituents are potentially better anti-cancer agents as compared to other phytoconstituents analysed in the current study. The interactions like hydrogen bonds, hydrophobic bonds, salt bridges and the interacting amino acid residues are shown (Table 7; Fig. 5).

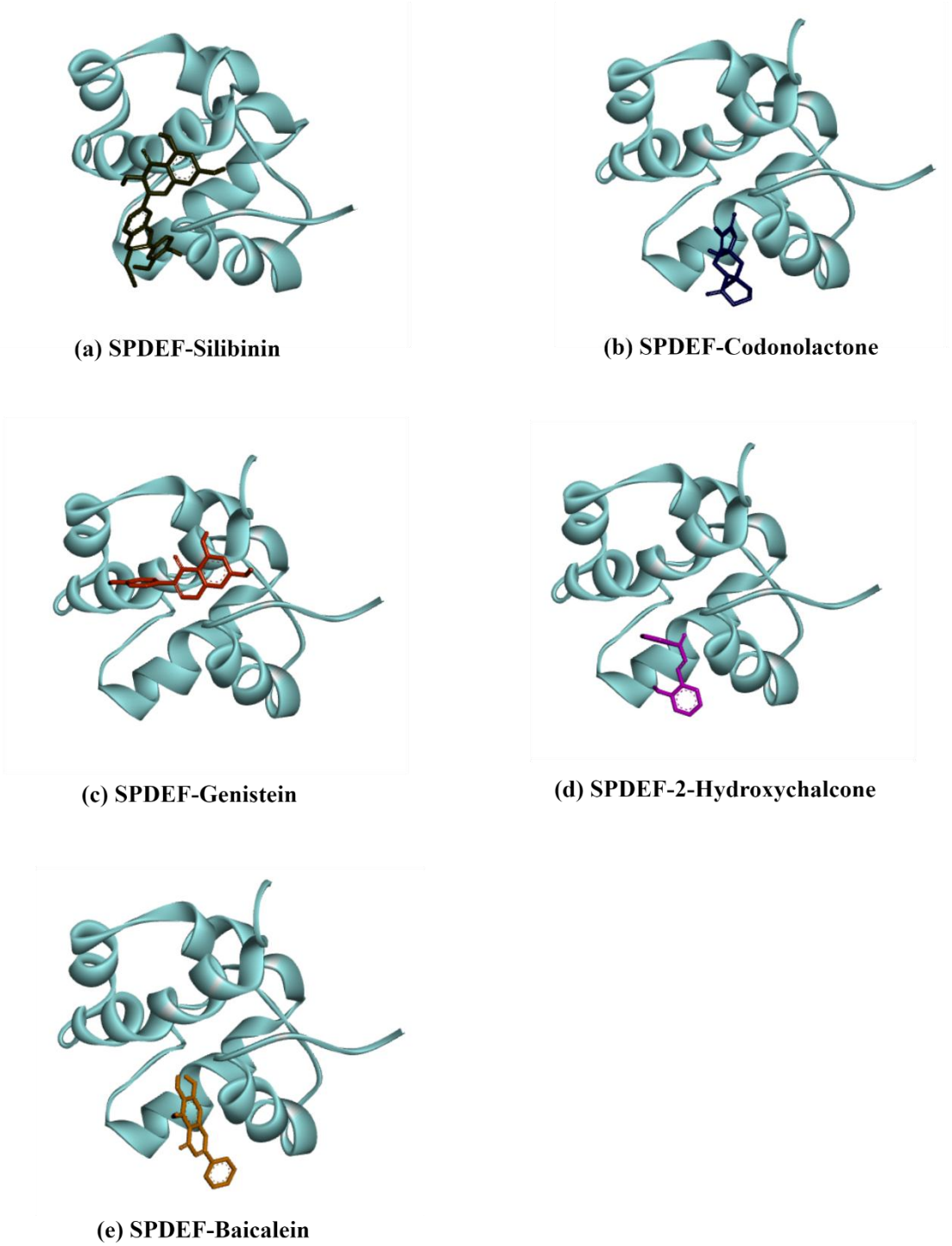

Fig. 6: 3-D view of the interaction between ligand (phytoconstituents) and target protein (SPDEF) by using Biovia Discovery Studio. The 3-D structure of SPDEF protein is shown in blue color and the ligands (phytoconstituents) are shown in different colors. Only the best five complexes, based on binding energy values, are represented here. The alphabets a-e stand for (a) SPDEF-Silibinin, (b) SPDEF-Codonolactone, (c) SPDEF-Genistein, (d) SPDEF-2-Hydroxychalcone and (e) SPDEF-Baicalein. These figures were produced by using the .pdb files of individual protein-ligand complexes generated in PyRx. The .pdb files were uploaded into Biovia Discovery Studio software.

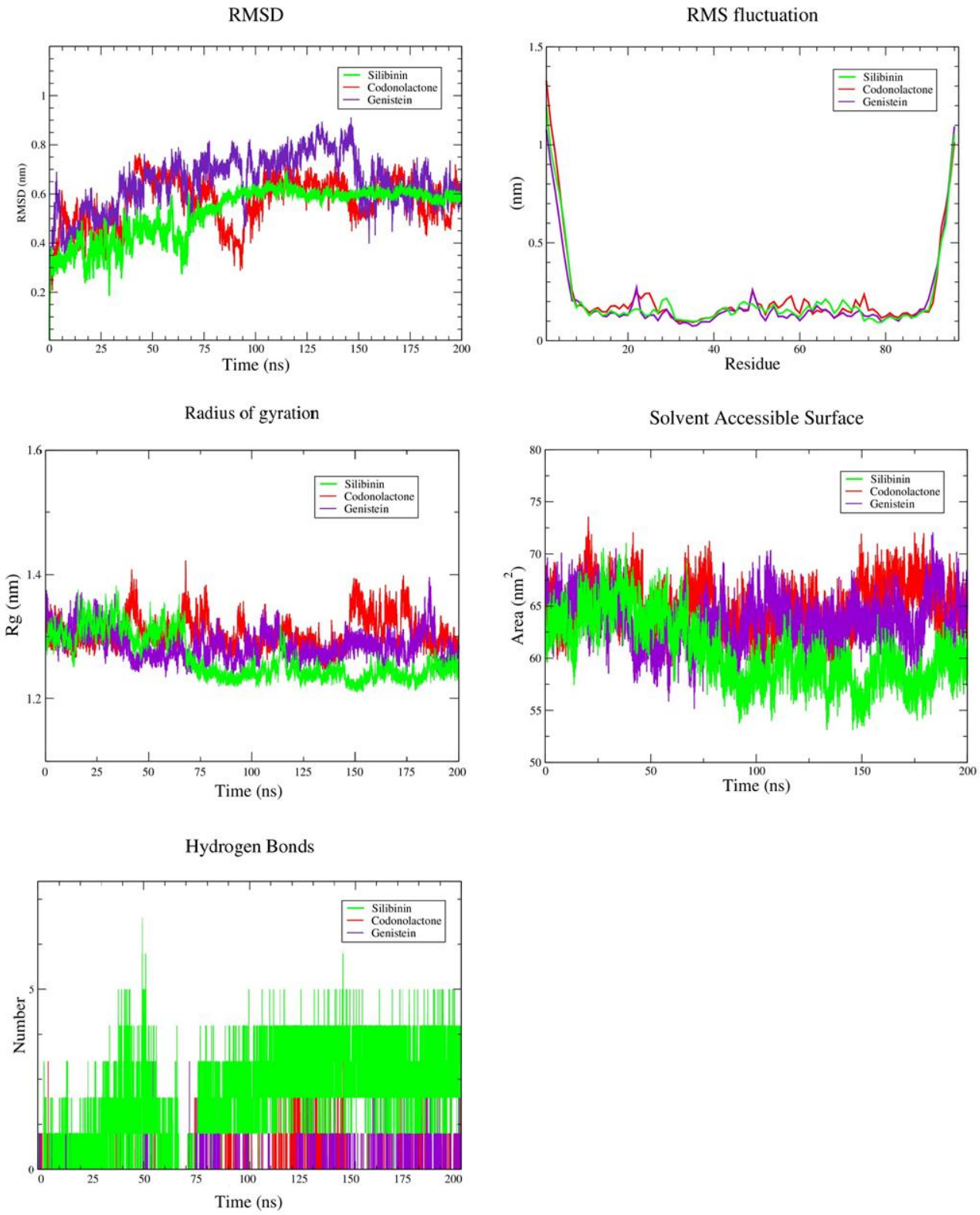

Fig. 7: Molecular dynamic simulation (A) Root mean square deviation (RMSD) for protein backbone and protein-ligand complex. (B) Root mean square fluctuation throughout the individual protein residues flexibility (C) Radius of Gyration shows the compactness of complex structure. (D) Solvent Accessible Surface Area (E) Hydrogen bond comparison of silibinin, codonolactone and genistein complexes. The behavior of protein-ligand complexes was studied at the atomic level using molecular dynamics simulations in GROMACS version 2021.3 package. 200 ns of simulation time were used in the production run with the Leap-frog MD integrator. The Graphs representing root mean square deviation (RMSD), root mean square fluctuation (RMSF), solvent accessible surface area (SASA) and radius of gyration (RoG) were computed.

Table 7
Using the .pdb files of individual protein-ligand complexes generated in PLIP

S.N.	Phytoconstituents	Hydrogen bond interaction	Hydrophobic interaction and other interaction
1	Silibinin	SER-5A, ASP-10A, SER-88A	ASP-10A, ILE-11A, ALA-89A
2	Codonolactone	TRP-38A, GLN-42A, HIS-82A, TRP-86A	ASP-10A, THR-13A, ALA-14A, HIS-82A
3	Genistein	SER-5A, SER-88A	LEU-8A, ILE-85A, ALA-89A
4	2-Hydroxychalcone	GLN-42A, TRP-86A	THR-13A, ALA-14A, ILE-85A, TRP-38A
5	Baicalein	ASP-10A, HIS-82A, TRP-86A	ASP-10A, THR-13A, ALA-14A, TRP-38A
6	Calycosin	SER-5A, ASP-84A, SER-88A	LEU-8A, ALA-89A
7	Fisetin	TRP-86A	ALA-14A, TRP-38A, ILE-85A
8	2-Methylanthraquinone		LEU-8A, ILE-85A, ALA-89A, PRO-93A
9	Curcumin	ASP-10A, TRP-38A, HIS-82A	ASP-10A, ILE-11A, ILE-85A
10	Icaritin	LYS-34A	GLN-33A, LYS-34A, LEU-36A, LEU-37A, GLN-53A
11	Noscapine	TRP-86A	ILE-85A, HIS-82A,
12	Scopoletin	SER-5A, SER-88A	LEU-8A, ALA-89A
13	Catechol	TRP-38A, GLN-42A, HIS-82A, TRP-86A	ASP-10A, TRP-86A
14	Ajoene	TRP-38A, GLN-42A,	ASP-10A, ILE-11A, LEU-17A, TRP-38A, TRP-86A
15	Allicin	TRP-38A, GLN-42A	ILE-11A, THR-13A, ALA-14A, TRP-38A

The lower binding energies predicted for compounds silibinin, codonolactone and genistein indicated that they fit well in the binding pocket of the human SPDEF forming a stable inhibitor-protein complex and also indicated no toxicity. The docked position of the top five phytoconstituents (based on the binding energy) with SPDEF, generated through the Biovia Discovery Studio is shown (Fig. 6).

Molecular Dynamics and Simulations: The stability of the optimal ligand-receptor pose under solvent conditions was investigated at the atomic level. Three ligands silibinin -7.7 kcal/mol, codonolactone -6.1 kcal/mol and genistein -6.1 kacl/mol demonstrated favorable binding energies. To assess structural stability, a 200 ns molecular dynamics simulation was conducted for each ligand. In RMSD analysis, silibinin exhibited the most stable structure, maintaining stability from ~75 ns to the end of the simulation while codonolactone achieved stability around 90 ns with fluctuations and genistein showed loop stability (Fig. 7A).

The average RMSD values for the silibinin 0.524486303, codonolactone 0.647715601 and genistein 0.569822986 were reported whereas the appropriate RMSD values for silibinin, codonolactone and genistein were 1.863 Å, 1.936 Å and 2.057Å respectively. The acceptable range for the appropriate RMSD value is below 3.0Å[33]. These results indicate the stability of the complex structure.

Residue flexibility was assessed using root mean square fluctuation (RMSF) analysis (Fig. 7B), revealing major fluctuations in loop regions at the protein's start (Gly1 to Ser5) and terminal side (Pro93 to Gly96). Notably, binding site residues including Gly7, Asp10, His82, Ile85, Ser88 and Ala89, residues exhibited positive fluctuations and maintained stability in the complex structure, with silibinin showing the least fluctuation.

Furthermore, the Radius of Gyration (RoG) analysis demonstrates that the silibinin complex structure achieved compactness earlier from ~75-80 ns in comparison to codonolactone which shows compactness from ~150 ns and genistein shows compactness from ~125 ns (Fig. 7C). A comparative analysis between silibinin, codonolactone and genistein from Radius of Gyration and Solvent Accessible Surface Area confirmed the consistency and accuracy of the simulation results (Fig. 7D). Hydrogen bond analysis (H-Bond) (Fig. 7E) provided insights into the number of hydrogen bonds formed in the silibinin, codonolactone and genistein complexes, further supporting the stability and compactness of the protein-ligand complexes. Collectively, these findings validate the reliability of the molecular dynamic simulations.

According to the binding scores, silibinin exhibited the best inhibitory impact against SPDEF protein. The breast cancer target under investigation had a strong affinity for the chosen phytoconstituents, according to the molecular docking analysis.

For further *in vivo* and *in vitro* studies to find the best therapeutic efficacy and least toxicity, the current predictions regarding these phytoconstituents will be required. In general, the outcomes of our predictions could serve as significant inputs for future experimental research. Structural or physicochemical analysis of developing

compounds regarded to be oral drug candidates established their drug-likeness properties.

Conclusion

Conclusively, the pharmacokinetics, drug-likeness and toxicity profiles of fifteen phytoconstituents were investigated. Using *in silico* methods, the fifteen phytoconstituents identified from the different plants were predicted for their inhibitory actions against breast cancer via their interaction with SPDEF. All the fifteen phytoconstituents obeyed Lipinski's rule of five for oral availability which is common in natural products. Genistein, 2-hydroxychalcone, ajoene and allicin are free from any of the predicted toxicological endpoints. The results showed appropriate cLogP and logS values for 2 methylanthraquinone suggesting better absorption and less toxicity. Using molecular dynamics simulations, the best docked pose with the receptor was chosen to evaluate the small molecules' behaviour during a 200 ns production time span.

The protein-ligand complex structure was simulated for 200 ns, the root-mean-square deviation (RMSD) calculations indicated stability after ~75 ns for the silibinin complex structure. The complex protein-ligand structure's flexibility, compactness and stability were further validated using Root Mean Square Fluctuation, Radius of Gyration and Solvent Accessible Surface respectively. The silibinin-receptor complex structure qualifies the maximum parameters in this study. Based on the analyses performed in the current study it is suggested that silibinin, codonolactone and genistein can be potentially good therapeutic agents for the treatment of breast cancer.

Acknowledgement

The authors want to acknowledge the Department of Bioinformatics, Central University of South Bihar, Gaya Bihar and the Indian Council of Medical Research, New Delhi, India for all technical support. The authors also acknowledge the National Supercomputing Mission (NSM) for providing computing resources for 'PARAM Ananta' at IIT Gandhinagar, which was implemented by C-DAC and supported by the Ministry of Electronics and Information Technology (MeitY) and the Department of Science and Technology (DST), Government of India.

References

1. Aboushanab A.R., El-Moslemany R.M., El-Kamel A.H., Mehanna R.A., Bakr B.A. and Ashour A.A., Targeted fisetin-encapsulated β-cyclodextrin Nanosponges for breast cancer, *Pharmaceutics*, **15(5)**, 1480 **(2023)**

2. Abraham M.J., Murtola T., Schulz R., Pall S., Smith J.C., Hess B. and Lindahl E., GROMACS: High performance molecular simulations through multi-level parallelism from laptops to supercomputers, *SoftwareX*, **1-2**, 19-25 **(2015)**

3. Acharya R., Chacko S., Bose P., Lapenna A. and Pattanayak S.P., Structure based multitargeted molecular docking analysis of selected furanocoumarins against breast cancer, *Sci Rep*, **9(1)**, 1-13 **(2019)**

4. Ahmad A., Wang Z., Ali R., Maitah M.Y., Kong D., Banerjee S., Padhye S. and Sarkar F.H., Apoptosis- inducing effect of garcinol is mediated by NF- κb signaling in breast cancer cells, *Journal of Cellular Biochemistry*, **109(6)**, 1134-1141 **(2010)**

5. Ahmed M., Lalloo F., Howell A. and Evans D., Risks of contralateral breast cancer in BRCA1 and BRCA2 mutation carriers, *Breast Cancer Research*, **12(S1)**, 14 **(2010)**

6. Allen M.P. and Tildesley D.J., Computer Simulation of Liquids, Oxford University Press **(2017)**

7. Almatroodi S.A., Almatroudi A., Khan A.A., Alhumaydhi F.A., Alsahli M.A. and Rahmani A.H., Potential therapeutic targets of Epigallocatechin gallate (EGCG), the most abundant Catechin in green tea and its role in the therapy of various types of cancer, *Molecules*, **25(14)**, 3146 **(2020)**

8. Andersen H.C., Molecular dynamics simulations at constant pressure and/or temperature, *The Journal of Chemical Physics*, **72(4)**, 2384-2393 **(1980)**

9. Ankit P.K., Manish P., Amit K.D., Vishant P. and Darshan P., Antitubercular, Antimalarial Activity and Molecular Docking Study of New Synthesized 7-Chloroquinoline Derivatives, *Polycyclic Aromatic Compounds*, **42**, 1-9 **(2021)**

10. Arnold M., Morgan E., Rumgay H., Da Costa A.M., Singh D., Laversanne M., Vignat J., Gralow J.R., Cardoso F., Siesling S. and Soerjomataram I., Current and future burden of breast cancer: Global statistics for 2020 and 2040, *The Breast*, **66**, 15-23 **(2022)**

11. Arnott J.A. and Planey S.L., The influence of lipophilicity in drug discovery and design, *Expert Opin Drug Discov*, **7**, 863-875 **(2012)**

12. Banerjee P., Eckert A.O., Schrey A.K. and Preissner R., ProTox-II: A webserver for the prediction of toxicity of chemicals, *Nucleic Acids Research*, **46(W1)**, 257-263 **(2018)**

13. Bekker H., Berendsen H. and Dijkstra E.J., Gromacs: a parallel computer for molecular dynamics simulations, *Science Open Phys Comput*, **92**, 252-256 **(1993)**

14. Bitew M., Desalegn T., Demissie T.B., Belayneh A., Endale M. and Eswaramoorthy R., Pharmacokinetics and drug-likeness of antidiabetic flavonoids: Molecular docking and DFT study, *PLOS ONE*, **16(12)**, e0260853 **(2021)**

15. Boado R.J., Blood–brain barrier genomics. Blood-Brain Barrier, Cite this article as Cold Spring, *Harb Perspect Biol*, **7**, 401-418 **(2015)**

16. Buchwalter G., Hickey M., Cromer A., Selfors L., Gunawardane R., Frishman J., Jeselsohn R., Lim E., Chi D., Fu X., Schiff R., Brown M. and Brugge J., PDEF promotes luminal differentiation and acts as a survival factor for ER-positive breast cancer cells, *Cancer Cell*, **23(6)**, 753-767 **(2013)**

17. Burley S.K., Berman H.M., Kleywegt G.J., Markley J.L., Nakamura H. and Velankar S., Protein data bank (PDB): The single

global macromolecular structure archive, *Methods in Molecular Biology*, **1607**, 627-641 **(2017)**

18. Chang H. et al, Synergistic anti-oral cancer effects of UVC and methanolic extracts of Cryptocarya concinna roots via apoptosis, oxidative stress and DNA damage, *International Journal of Radiation Biology*, **92(5)**, 263-272 **(2016)**

19. Chen C., Chen C., Huang C. and Chang Y., Evaluating molecular properties involved in transport of small molecules in stratum Corneum: A quantitative structure-activity relationship for skin permeability, *Molecules*, **23(4)**, 911 **(2018)**

20. Cho S., Ryu J. and Surh Y., Ajoene, a major Organosulfide found in crushed garlic, induces NAD(P)H: quinone Oxidoreductase expression through nuclear factor E2-related factor-2 activation in human breast epithelial cells, *Journal of Cancer Prevention*, **24(2)**, 112-122 **(2019)**

21. Choong E., Dobrinas M., Carrupt P. and Eap C.B., The permeability P-glycoprotein: A focus on enantioselectivity and brain distribution, *Expert Opinion on Drug Metabolism & Toxicology*, **6(8)**, 953-965 **(2010)**

22. Clark D.E., Rapid calculation of polar molecular surface area and its application to the prediction of transport phenomena prediction of intestinal absorption, *Journal of Pharmaceutical Sciences*, **88(8)**, 807-14 **(1999)**

23. Criscitiello C. and Corti C., Breast cancer genetics: Diagnostics and treatment, *Genes*, **13(9)**, 1593 **(2022)**

24. Daina A., Michielin O. and Zoete V., SwissADME: A free web tool to evaluate pharmacokinetics, drug-likeness and medicinal chemistry friendliness of small molecules, *Scientific Reports*, **7(1)**, 42710-42717 **(2017)**

25. DeLano W.L., Pymol: An open-source molecular graphics tool, *CCP4 Newsl Protein Crystallogr*, **40(1)**, 82-92 **(2002)**

26. Doddapaneni R., Patel K., Chowdhury N. and Singh M., Reversal of drug-resistance by noscapine chemo-sensitization in docetaxel resistant triple negative breast cancer, *Scientific Reports*, **7(1)**, 15824 **(2017)**

27. Feldman R.J., Sementchenko V.I., Gayed M., Fraig M.M. and Watson D.K., Pdef expression in human breast cancer is correlated with invasive potential and altered gene expression, *Can Res*, **63**, 4626-4631 **(2003)**

28. Hakkola J., Hukkanen J., Turpeinen M. and Pelkonen O., Inhibition and induction of CYP enzymes in humans: An update, *Archives of Toxicology*, **94(11)**, 3671-3722 **(2020)**

29. Hollenberg P.F., Characteristics and common properties of inhibitors, inducers and activators of CYP enzymes, *Drug Metabolism Reviews*, **34(1-2)**, 17-35 **(2002)**

30. Joshi T., Sharma P., Pundir H. and Chandra S., *In silico* identification of natural fungicide from Melia azedarach against isocitrate lyase of Fusarium graminearum, *J Biomol Struct Dyn*, **39(13)**, 1-19 **(2020)**

31. Kapinova A., Stefanicka P., Kubatka P., Zubor P., Uramova S., Kello M., Mojzis J., Blahutova D., Qaradakhi T., Zulli A., Caprnda M., Danko J., Lasabova Z., Busselberg D. and Kruzliak P., Are plant-based functional foods better choice against cancer than single phytochemicals? A critical review of current breast cancer research, *Biomedicine & Pharmacotherapy*, **96**, 1465-1477 **(2017)**

32. Khan M.I., Bouyahya A., Hachlafi N.E., Menyiy N.E., Akram M., Sultana S., Zengin G., Ponomareva L., Shariati M.A., Ojo O.A., Dall'Acqua S. and Elebiyo T.C., Anticancer properties of medicinal plants and their bioactive compounds against breast cancer: A review on recent investigations, *Environmental Science and Pollution Research*, **29(17)**, 24411-24444 **(2022)**

33. Kufareva I. and Abagyan R., Methods of protein structure comparison, *Methods in Molecular Biology*, **857**, 231-257 **(2011)**

34. Lipinski C.A., Lombardo F., Dominy B.W. and Feeney P.J., Experimental and computational approaches to estimate solubility and permeability in drug discovery and development settings, *Advanced Drug Delivery Reviews*, **23(1-3)**, 3-25 **(1997)**

35. Liu Z., Liu M., Liu M. and Li J., Methylanthraquinone from Hedyotis diffusa WILLD induces ca2+-mediated apoptosis in human breast cancer cells, *Toxicology in Vitro*, **24(1)**, 142-147 **(2010)**

36. Liu Z., Yang C., Zhang L., Yang C. and Xu X., Baicalein, as a Prooxidant, triggers mitochondrial Apoptosis in MCF-7 human breast cancer cells through mobilization of intracellular copper and reactive oxygen species Generation, *OncoTargets and Therapy*, **12**, 10749-10761 **(2019)**

37. Maitisha G., Aimaiti M., An Z. and Li X., Allicin induces cell cycle arrest and apoptosis of breast cancer cells in vitro via modulating the p53 pathway, *Molecular Biology Reports*, **48(11)**, 7261-7272 **(2021)**

38. Molinspiration Cheminformatics, Calculation of Molecular Properties and Bioactivity Score, http://www.molinspiration.com/cgi-bin/properties, Accessed 8th December 2020 **(2020)**

39. Mukhopadhyay A., Khoury T., Stein L., Shrikant P. and Sood A.K., Prostate derived Ets transcription factor and Carcinoembryonic antigen related cell adhesion molecule 6 constitute a highly active oncogenic axis in breast cancer, *Oncotarget*, **4(4)**, 610-621 **(2013)**

40. Nose S., A molecular dynamics method for simulations in the canonical ensemble, *Molecular Physics*, **100(1)**, 191-198 **(2002)**

41. Orrantia-Borunda E., Anchondo-Nunez P., Acuna-Aguilar L.E., Francisco O.G. and Claudia A.R., Subtypes of Breast Cancer, In Mayrovitz H.N., eds., Breast Cancer, Brisbane (AU), Exon Publications, Chapter 3 **(2022)**

42. Pujari I., Sengupta R. and Babu V.S., Docking and ADMET studies for investigating the anticancer potency of Moscatilin on APC10/DOC1 and PKM2 against five clinical drugs, *Journal of Genetic Engineering and Biotechnology*, **19(1)**, 161 **(2021)**

43. Raies A.B. and Bajic V.B., *In silico* toxicology: computational methods for the prediction of chemical toxicity, Wiley Interdiscip., *Rev. Comput Mol Sci*, **6**, 147-172 **(2016)**

44. Raju L., Lipin R. and Eswaran R., Identification, ADMET evaluation and molecular docking analysis of phytosterols from

Banaba (Lagerstroemia speciosa (L.) Pers) seed extract against breast cancer, *In Silico Pharmacology*, **9(1)**, 43 **(2021)**

45. Sadeghi M., Moradi M., Madanchi H. and Johari B., *In silico* study of garlic (Allium sativum L.) derived compounds molecular interactions with α-glucosidase, *In Silico Pharmacology*, **9(1)**, 1-8 **(2021)**

46. Sharma R., Descriptive epidemiology of incidence and mortality of primary liver cancer in 185 countries: Evidence from GLOBOCAN 2018, *Japanese Journal of Clinical Oncology*, **50(12)**, 1370-1379 **(2020)**

47. Shukla Abhimati and Singh Lalit Kumar, A comparative study on the removal and recovery of hexavalent chromium from tannery wastewater using an isolated strain *Aspergillus proliferans* LA and a known strain *Aspergillus terreus*, *Res. J. Chem. Environ.*, **27(11)**, 97-109 **(2023)**

48. Sultana R., Molecular docking based virtual screening of the breast cancer target NUDT5, *Bioinformation*, **15(11)**, 784-789 **(2019)**

49. Talib W.H., Al-hadid S.A., Wild Ali M.B., AL-Yasari I.H. and Abd Ali M.R., Role of curcumin in regulating p53 in breast cancer: An overview of the mechanism of action, *Breast Cancer: Targets and Therapy*, **10**, 207-217 **(2018)**

50. Toshikiro K. and Kazutaka H., Gastrointestinal transit and drug absorption, *Biol Pharm Bull*, **25(2)**, 149-64 **(2002)**

51. Trott O. and Olson A.J., AutoDock Vina: improving the speed and accuracy of docking with a new scoring function, efficient optimization and multithreading, *J Comput Chem*, **31(2)**, 455-461 **(2009)**

52. Turner D.P., Moussa O., Sauane M., Fisher P.B. and Watson D.K., Prostate-derived ETS factor is a mediator of metastatic potential through the inhibition of migration and invasion in breast cancer, *Cancer Research*, **67(4)**, 1618-1625 **(2007)**

53. Uchida S. and Sugino T., *In Silico* identification of genes associated with breast cancer progression and prognosis and novel therapeutic targets, *Biomedicines*, **10(11)**, 2995 **(2022)**

54. Van Waterschoot R.A. and Schinkel A.H., A critical analysis of the interplay between cytochrome P450 3A and P-glycoprotein: recent insights from knockout and transgenic mice, *Pharmacological Reviews*, **63(2)**, 390410 **(2011)**

55. Vanommeslaeghe K., Hatcher E., Acharya C., Kundu S., Zhong S., Shim J., Darian E., Guvench O., Lopes P., Vorobyov I. and Mackerell A.D., CHARMM general force field: A force field for drug- like molecules compatible with the CHARMM all- atom additive biological force fields, *Journal of Computational Chemistry*, **31(4)**, 671-690 **(2009)**

56. Veber D.F., Johnson S.R., Cheng H.Y., Smith B.R., Ward K.W. and Kopple K.D., Molecular properties that influence the oral bioavailability of drug candidates, *J Med Chem*, **45(12)**, 2615-2623 **(2002)**

57. Wang W., Chen B., Zou R., Tu X., Tan S., Lu H., Liu Z. and Fu J., Codonolactone, a sesquiterpene lactone isolated from Chloranthus henryi Hemsl, inhibits breast cancer cell invasion, migration and metastasis by downregulating the transcriptional activity of Runx2, *International Journal of Oncology*, **45(5)**, 1891-1900 **(2014)**

58. Wang X., Zheng N., Dong J., Wang X., Liu L. and Huang J., Estrogen receptor-α36 is involved in icaritin induced growth inhibition of triple-negative breast cancer cells, *The Journal of Steroid Biochemistry and Molecular Biology*, **171**, 318-327 **(2017)**

59. Wasidi Al, Hassan A.S. and Naglah A.M., *In vitro* cytotoxicity and drug likeness of pyrazolines and pyridines bearing benzofuran moiety, *Journal of Applied Pharmaceutical Science*, **10(4)**, 142-148 **(2020)**

60. Wing Y.C.C, Gibbons N., Wayne J.D. and Lawrence N.D., Silibinin – A promising new treatment for cancer, *Anti-Cancer Agents in Medicinal Chemistry*, **10(3)**, 186-195 **(2010)**

61. Ye T., Feng J., Wan X., Xie D. and Liu J., Double agent: SPDEF Gene with both oncogenic and tumor-suppressor functions in breast Cancer, *Cancer Management and Research*, **12**, 3891-3902 **(2020)**

62. Yu N., Li N., Wang K., Deng Q., Lei Z., Sun J. and Chen L., Design, synthesis and biological activity evaluation of novel scopoletin-NO donor derivatives against MCF-7 human breast cancer *in vitro* and *in vivo*, *European Journal of Medicinal Chemistry*, **224**, 113701 **(2021)**

63. Zhou R., Chen H., Chen J., Chen X., Wen Y. and Xu L., Extract from astragalus membranaceus inhibit breast cancer cells proliferation via PI3K/AKT/mTOR signaling pathway, *BMC Complementary and Alternative Medicine*, **18(1)**, 83 **(2018)**

64. Zoete V., Cuendet M.A., Grosdidier A. and Michielin O., SwissParam: A fast force field generation tool for small organic molecules, *Journal of Computational Chemistry*, **32(11)**, 2359-2368 **(2011)**.

(Received 02nd March 2024, accepted 04th April 2024)